ACCOUNTS
of chemical research

Iodine/Iodide-Free Dye-Sensitized Solar Cells

SHOZO YANAGIDA,* YOUHAI YU, AND KAZUHIRO MANSEKI

Center for Advanced Science and Innovation, Osaka University, Yamadaoka 2-1, Suita, Osaka, 565-0871 Japan

RECEIVED ON MARCH 2, 2009

CONSPECTUS

Dye-sensitized solar cells (DSSCs) are built from nanocrystalline anatase TiO_2 with a 101 crystal face (nc-TiO_2) onto which a dye is absorbed, ruthenium complex sensitizers, fluid I^-/I_3^- redox couples with electrolytes, and a Pt-coated counter electrode. DSSCs have now reached efficiencies as high as 11%, and G24 Innovation (Cardiff, U.K.) is currently manufacturing them for commercial use. These devices offer several distinct advantages. On the basis of the electron lifetime and diffusion coefficient in the nc-TiO_2 layer, DSSCs maintain a diffusion length on the order of several micrometers when the dyed-nc-TiO_2 porous layer is covered by redox electrolytes of lithium and/or imidazolium iodide and their polyiodide salts. The fluid iodide/iodine (I^-/I_3^-) redox electrolytes can infiltrate deep inside the intertwined nc-TiO_2 layers, promoting the mobility of the nc-TiO_2 layers and serving as a hole-transport material of DSSCs. As a result, these materials eventually give a respectable photovoltaic performance.

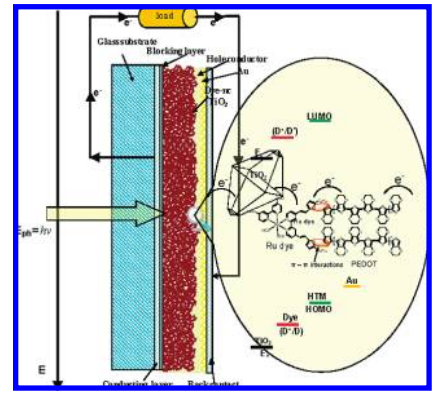

On the other hand, fluid I^-/I_3^- redox shuttles have certain disadvantages: reduced performance control and long-term stability and incompatibility with some metallic component materials. The I^-/I_3^- redox shuttle shows a significant loss in short circuit current density and a slight loss in open circuit voltage, particularly in highly viscous electrolyte-based DSSC systems. Iodine can also act as an oxidizing agent, corroding metals, such as the grid metal Ag and the Pt mediator on the cathode, especially in the presence of water and oxygen. In addition, the electrolytes (I^-/I_3^-) can absorb visible light ($\lambda = \sim$430 nm), leading to photocurrent loss in the DSSC. Therefore, the introduction of iodide/iodine-free electrolytes or hole-transport materials (HTMs) could lead to cost-effective alternatives to TiO_2 DSSCs.

In this Account, we discuss the iodide/iodine-free redox couple as a substitute for the fluid I^-/I_3^-redox shuttle. We also review the adaptation of solid-state HTMs to the iodide/iodine-free solid-state DSSCs with an emphasis on their pore filling and charge mobility in devices and the relationship of those values to the performance of the resulting iodide/iodine-free DSSCs. We demonstrate how the structures of the sensitizing dye molecules and additives of lithium or imidazolium salts influence device performance. In addition, the self-organizing molecular interaction for electronic contact of HTMs to dye molecules plays an important role in unidirectional charge diffusion at interfaces. The poly(3,4-ethylenedioxythiophene) (PEDOT)-based DSSCs, which we obtain through photoelectrochemical polymerization (PEP) using 3-alkylthiophen-bearing ruthenium dye, HRS-1, and bis-EDOT, demonstrates the importance of nonbonding interface contact (e.g., $\pi-\pi$-stacking) for the successful inclusion of HTMs.

1. Introduction

Dye-sensitized solar cells (DSSCs) are constructed with dye-absorbed nanocrystalline anatase TiO_2 with a 101 crystal face (nc-TiO_2), ruthenium complex sensitizers, electrolyte containing fluid I^-/I_3^- redox couples, and Pt-coated counter electrode.[1] They have excellent performance with respectable up to 11% conversion efficiency, which can be rationalized by the following five factors as reviewed in our recent review article.[2] (1) The energetics of the conduction band of nc-TiO_2 matches the potential of photoformed electrons from both singlet and triplet states of Ru complexes,[3] leading to respectable incident photocurrent

Published on the Web 10/30/2009 www.pubs.acs.org/acr
10.1021/ar900069p CCC: $71.50

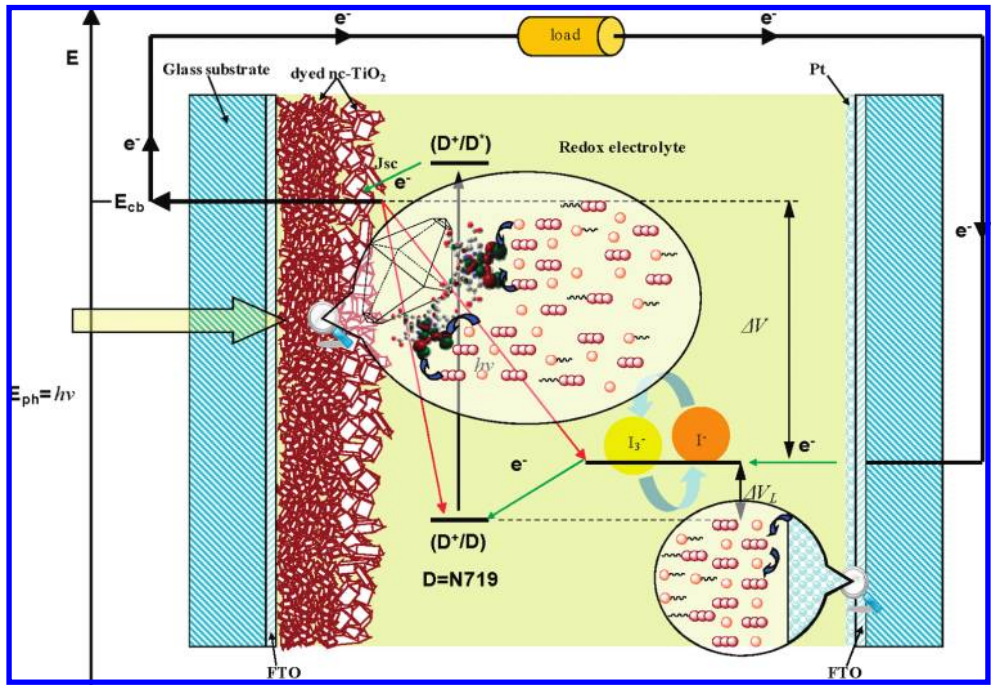

FIGURE 1. Mechanistic drawing of iodide/iodine redox (I^-/I_3^-) shuttle in DSSC.

efficiency (IPCE) in the wide light energy region. (2) Effective electron diffusion coefficients reported for nc-TiO_2 are in the order of 10^{-6} cm^2 s^{-1} that is consistent with the high mobility of nc-TiO_2 in the order of $2.4-3 \times 10^{-4}$ cm^2 V^{-1} s^{-1}.[4] (3) The lifetime of electrons in nc-TiO_2 layers gives a subsecond order of electron lifetime, leading to large diffusion length ($\sim$20 μm) of nc-TiO_2 layers when coupled with respectable diffusion coefficients. (4) The conductivity of fluid iodide/iodine electrolytes is high enough owing to ion exchange mechanism (so-called Grotthuss mechanism).[5] (5) Infiltration of the fluid electrolyte into porous nc-TiO_2 layer anodes is due to the fluidity of the electrolyte itself. In fact, remarkable conversion efficiencies (more than 10%)[6] have been reported, where the adsorption of sensitizing dye molecules is controlled on nc-TiO_2 and their optical and photophysical properties are optimized from viewpoints of collection of wide-range solar light energy.

In order to make DSSCs fit to practical outdoor use as a next generation photovoltaic, we must take into account long-term durability of DSSC modules as well as their optimized conversion efficiency and cost-effectiveness using environmentally friendly materials. The standardized packing durability test for solar cell modules itemizes the damp heat stability at 85 °C under 85% humidity as the most severe durability evaluation. It is known that iodine is corrosive to metallic grids such as silver in the presence of break-in water and oxygen. However, the Fujikura Ltd. Japan group confirmed that their DSSC modules (conversion efficiency of 5%) are durable at 85 °C under 85% humidity when they employed robust films for covering grid metals on anodes fluorine-doped tin oxide (FTO) and a double sealing (chemical adhesion and physical pressure) of the modules.[7] Their success may suggest that, when iodine-free nonvolatile and noncorrosive electrolytes are replaced as a substitute of fluid I^-/I_3^- electrolytes, the long-term stability and reliability of a DSSC module could be accomplished much favorably and cost-effectively by direct usage of silver metal as grid and aluminum foil as cathode substrates.

In this Account, iodide/iodine-free redox electrolytes and hole-transport materials (HTMs) applied to DSSCs are reviewed, and iodide/iodine-free DSSCs using poly(3,4-ethylenedioxythiophene) (PEDOT) as HTM layers will also be the focus in view of nanopore filling by *in situ* photoelectrochemical polymerization (PEP), charge diffusion in the devices, and nonbonding molecular organization at interfaces of dye molecules and PEDOT on nc-TiO_2.

2. Iodide/Iodine-Free Redox Couple Shuttle as Electrolytes of DSSCs

The key function of I^-/I_3^- electrolytes in DSSCs is to transfer electrons to the oxidized ruthenium dye molecules that are formed photochemically via electron injection into nc-TiO_2, completing the internal electrochemical circuit between the photoanode and the counter cathode (Figure 1). In the stationary state, the electron-deficient and larger-size polyiodide

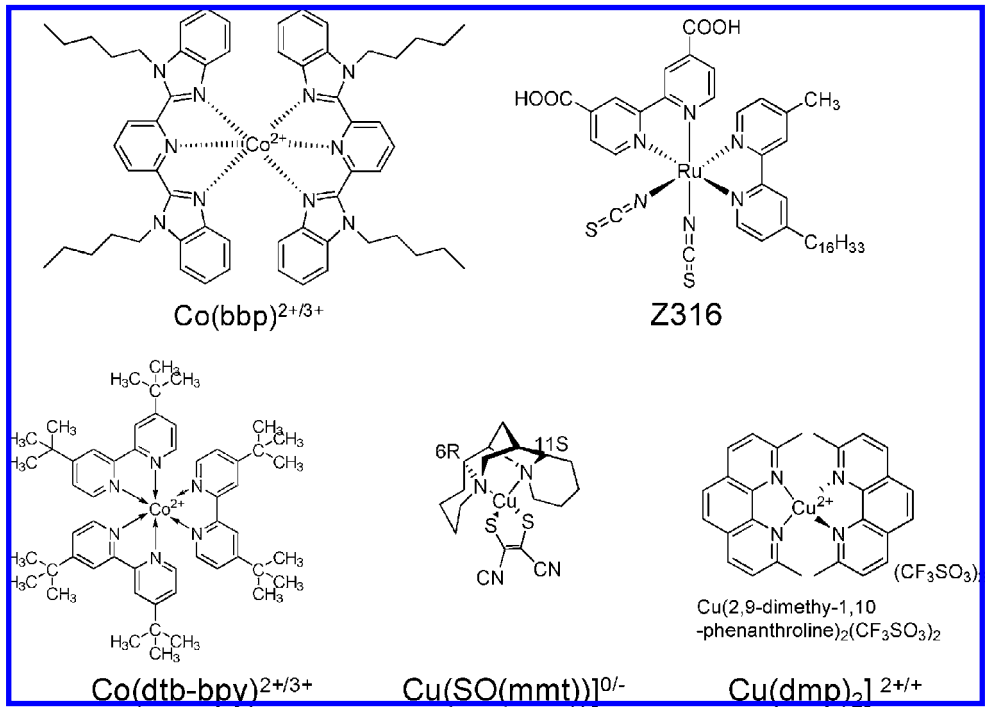

FIGURE 2. Metal complexes of redox shuttles and an effective sensitizer.

species exemplified by triiodide ions (I_3^-) may have a concentration gradient near interfaces of dyed nc-TiO_2 layers, especially in high-boiling-point-solvent-based and ionic-liquid-based DSSCs, and unfavorable charge recombination should occur between them with high probability in such electrolyte solvents.[8] Such intrinsic nonbonding interaction can be explained as being due to weak interaction through electron-rich parts in the ruthenium dyes designated as the highest occupied molecular orbital (HOMO) located on the SCN group and electron-poor sites designated as the lowest occupied molecular orbital (LUMO) of triiodide. Thus, the I^-/I_3^- redox couple shuttle of DSSCs is depicted in Figure 1 using the molecular orbital of the ruthenium N3 dye molecule in part.[9] The I^-/I_3^- redox couple should play an essential role in the dye molecules on nc-TiO_2 when the dye molecules are photoexcited on nc-TiO_2 and the iodide ion (I^-) is oxidized in the vicinity, and the resulting triiodide (I_3^-) ions are reduced to I^- ions at the cathode as depicted in Figure 1.

Grätzel's group first reported charge-transfer dynamics of a new one-electron redox couple, cobalt(II)-bis[2,6-bis(1′-butylbenzimidazol-2′-yl)pyridine] (Co-bbp in Figure 2) in N-719-sensitized DSSC, revealing that it works as a redox couple in DSSC systems.[10] It was interesting to note that the photovoltaic cells fabricated using an acetonitrile/ethylene carbonate solution of this redox couple yielded the conversion efficiencies of 2.2% at 94% sun irradiation and 5.2% at 9.4% sun irradiation when the oleophilic ruthenium dye, Z316, was employed as a sensitizer (Figure 2). Bignozzi and his co-workers also introduced non-iodine DSSCs using a series of Co(II) and Co(III) complexes with substituted bipyridine ligands.[11] The best device was fabricated using the ruthenium N3 dye as a sensitizer and tris(4,4′-di-*tert*-butyl-2,2′-dipyridyl)-cobalt(II/III) perchlorate (Co-dtb-bpy in Figure 2) as a redox couple in γ-butyrolactone, giving only 1.3% conversion efficiency under one-sun conditions. Interestingly, the effect of lithium triflate ($LiCF_3SO_3$) on the performance was discussed in detail.

Three copper complexes shown in Figure 2 were examined as a substitute of the I^-/I_3^- redox couple.[12] They were successfully applied to iodide/iodine-free DSSCs that were sensitized with the ruthenium N-719 dye. The V_{oc} values of copper complexes increase in the order: $[Cu(phen)_2]^{2+/+}$ (0.57 V), $[Cu(SP)(mmt)]^{0/-}$ (0.66 V), and $[Cu(dmp)_2]^{2+/+}$ (0.79 V), in agreement with the order of the redox potentials of the copper complexes. The η values of DSSCs using $[Cu(phen)_2]^{2+/+}$, $[Cu(dmp)_2]^{2+/+}$, and $[Cu(SP)(mmt)]^{0/-}$ were determined as 1%, 1.4%, and 1.3%, respectively. Interestingly, the copper redox couples $Cu(dmp)_2{}^{2+/+}$ and $Cu(SP)(mmt)]^{0/-}$ gave 2.2 and 1.9%, respectively, under the weak solar light irradiation of 20 mW/cm^2 intensity. The decrease of the conversion efficiency under high light irradiation suggests that the charge-transporting ability of the redox shuttle is a crucial condition as well as the matching of the redox potential with dye energetics.

Two pseudohalogen redox couples, $(SeCN)_2/SeCN^-$ and $(SCN)_2/SCN^-$, which have redox potentials of, respectively, 190

and 430 mV more positive than the I^-/I_3^- couple, were investigated as redox shuttles in DSSCs.[13] With the ruthenium N_3 sensitizer, the maximum IPCE was 80%, 20%, and 4% for the I_3^-/I^-, $(SeCN)_2/SeCN^-$, and $(SCN)_2/SCN^-$ couples, respectively. Transient absorption spectroscopy demonstrated that the lower efficiencies were related to a slower dye regeneration rate when SCN^- or $SeCN^-$ was used instead of I^-.

3. Introduction of p-Type Semiconducting Materials

Careful investigation on limiting currents of the I^-/I_3^- redox couple using microelectrodes revealed that the charge diffusion coefficient is dependent on increasing concentrations of I^- and I_3^-. At the conventional concentration of the I^-/I_3^- redox shuttle in DSSC ($I^- = 0.60$ M, $I_2 = 0.03$ M), the charge diffusion in the I^-/I_3^- redox shuttle takes the course of charge diffusion mechanism; that is, migration of I^-/I_3^- is not dominant. The fact that gelled-electrolyte-based DSSC systems using low molecular gelling agents gave the same conversion efficiency of those without the gelling agents[8] may well explain this charge diffusion interpretation as well as the determination of exchange charge transport of the I^-/I_3^- redox couple using a microelectrode technique.[6] On the other hand, the electron diffusion in the nc-TiO_2 electrodes is identified as the minority carriers and the ionic mobility is unimportant.[14] The value of the electron diffusion coefficient ($\sim 10^{-4}$ cm^2 s^{-1}) depends on adsorbed cationic species such Li^+ and imidazolium cation from electrolytes[15] and further on the electron density in nc-TiO_2 anodes. Accordingly, the mesoporous nc-TiO_2 layer and the I^-/I_3^- redox shuttle can be regarded as electron-transporting and hole-transporting layers, respectively, and then the I^-/I_3^- redox shuttle as the electrolyte can be replaced by a p-type semiconducting material as a hole-transporting mediator.

3.1. Inorganic Hole-Transport Materials (HTMs). CuI is soluble in acetonitrile, and the solution was applied as a HTM to the solidification of DSSCs and works as a substitute of the liquid I^-/I_3^- redox couple. The efficiency of the fully solid-state CuI-based DSSC was improved from initial 1% to about 6% by Tennakone et al.[16] However, Sirimanne et al.[17] found that the deterioration of CuI-based solid-state DSSCs was rapid because the interface of TiO_2/CuI degrades due to the formation of a trace amount of Cu_2O and/or CuO with the release of iodine on standing. The authors had observed gradual growth of the nanosized CuI in the porous space of the DSSC, leading to the decrease of the performance of the fully solid-state CuI-based DSSC. Kumara et al. recently reported the use of crystal growth inhibitors for CuI-based DSSCs.[18]

CuSCN is an alternative to replace CuI with a more stable performance. O'Regan et al. developed an electrodeposition techique and achieved an overall energy conversion efficiency of 1.5%.[19] Kumara et al.[20] found that CuSCN can be deposited on Ru-dye-coated nc-TiO_2 layers by using *n*-propylsulfide as a solvent of CuSCN. Later, O'Regan et al.[21] improved the efficiency up to ca. 2% at one sun irradiation. On the other hand, recent attempts to apply p-type NiO particles to a hole-transporting layer resulted in very poor performance of an iodide/iodine-free DSSC.[22]

3.2. Organic Hole-Transport Materials. Since most of organic hole-transporting materials, either molecules or polymers (Figure 3), are soluble or dispersible in organic solvent, simple methods such as spin-coating or *in situ* electrochemical methods that may rely on electrophoresis, were attempted for pore filling of nanoporous nc-TiO_2 layers to fabricate iodide/iodine-free DSSCs.

3.2.1. Molecular Hole-Transport Materials (HTM). In 1998, Grätzel et al. reported the first efficient solid-state DSSC using 2,2′,7,7′-tetranis(*N*,*N*-di-*p*-methoxyphenyl-amine)9,9′-spirobifluorene (OMeTAD) as a low molecular organic HTM with N3 dye as a sensitizer.[23] The Spiro-OMeTAD-based DSSC (thickness ~ 2 μm) has been reviewed as a solid-state DSSC, and the respectable performance (ca. 4%) has been rationalized in view of electron transport through nc-TiO_2 layers and electron-hopping mechanism of the hole-transporting Spiro-OMeTAD. The unidirectional electron flow without charge recombination between electrons in the nc-TiO_2 and dye molecules was attributed to the additives, lithium bis-(trifluoromethylsulfone)amide (LiTFSI) and a Lewis salt $N(PhBr)_3SbCl_6$ as dopants that facilitate charge compensation and improve charge mobility of the OMeTAD-based DSSC.

Iodide/iodine-free DSSC was extended to conventional aryl amine derivatives as HTM. Although *N*,*N*′-diphenyl-*N*,*N*′-(*m*-tolyl)-benzidine (TPD) was previously reported to give poor results, the Grätzel group recently succeeded in applying tris-[4-(2-methoxy−ethoxy)-phenyl]-amine (TMEPA) as a HTM coupled with oleophilic K51 ruthenium dye as sensitizer and $NaBF_4$ and LiTFSI as dopants, obtaining power conversion efficiencies of up to 2.4% under simulated AM1.5 irradiation (100 mW cm^{-2}).[24]

3.2.2. Polymeric Hole-Transport Materials (HTM). Iodide/iodine-free DSSCs using conductive polymers such as polythiophene derivatives and polyaniline (PANI) derivatives were attempted to construct using a spin-coating technique and related dip-coating methods. At first, poly(3-butylth-

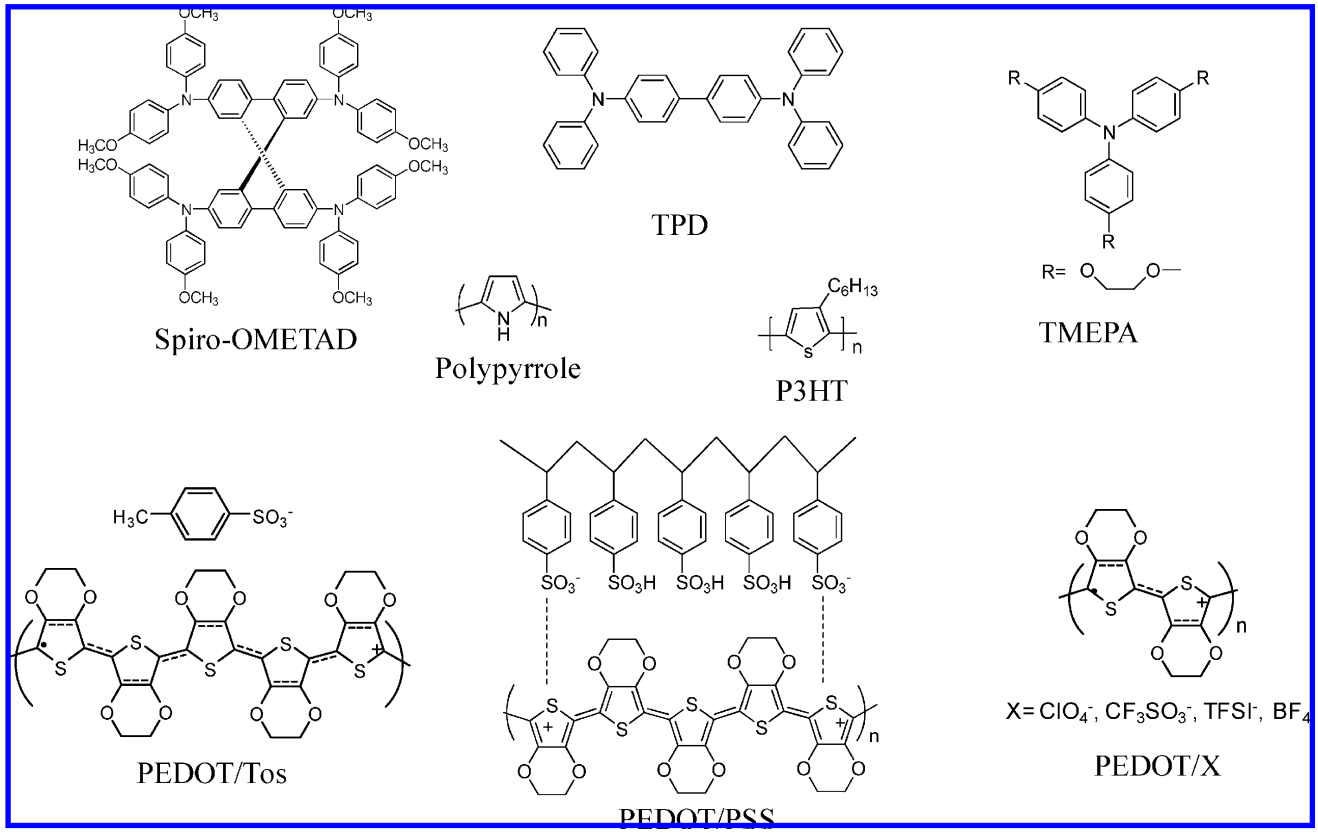

FIGURE 3. Organic HTMs investigated for non-iodine DSSCs.

iophene)[25] and poly(octylthiophene)[26] were examined using some organic dyes with no carboxyl groups or N3 dye as sensitizer, giving very poor results. Employment of poly(4-undecy-2,2′-bithiophene)[27] and poly(3-undecy-2,2′-bithiophene)[28] also resulted in giving poor performance with fill factor (ff = ~0.4) and short circuit current density (J_{sc} ~70 μA cm^{-2}) under comparable conditions. Recent attempts using regioregular poly(3-hexylthiophene) (P3HT) for hole-transport layers of N3 or N-719-sensitized DSSC led to slightly improved performances (η = ~0.8%).[29−31]

The authors recently succeeded in fabricating P3HT-based DSSCs with η = 2.70% under illumination with AM1.5 solar light irradiation.[32] Employment of very thin nc-TiO_2 layers (thickness ~ 400 nm) prepared using the spin-coating technique, oleophilic dye molecules such as HRS-1, and ionic liquid containing *t*-BP and LiTFSI as additives led to the success. Almost the same result has been reported using the organic dye D102 by Ramakrishna et al.[33]

With regards to polyaniline (PANI), the spin-coating technique using a PANI dispersion with high conductivity or electrochemical deposition of polyaniline gave very poor performance.[34]

3.3. Fabrication of PEDOT-Based DSSC. Poly(3,4-ethylenedioxythiophene) poly(styrenesulfonate) (PEDOT/PSS) is well-known to have a respectable wide range of conductivity (10^{-3}−500 S/cm), high level of transparency, and chemical and thermal stability with safe handling. PEDOT/PSS is now successfully applied to organic light emitting diodes and organic thin film solar cells as charge-transporting layers. Aqueous PEDOT/PSS dispersions have secondary and tertiary structures as nanosize particles ranging from 10 to 90 nm, and the conductivity seems to depend on the particle size and structures. The nanometer-sized pores of nc-TiO_2 layers (~30 nm) could not be filled deep inside by simple methods that normally rely on capillary force or gravity.

3.3.1. In Situ Photoelectrochemical Polymerization. Although micrometer-thick porous nc-TiO_2 electrodes that work as electron acceptors with respectable electron-transporting ability are the most important characteristics in DSSC devices, such nanoporous structures are the most difficult obstacle for polymeric HTM to infiltrate into the nanospace of nc-TiO_2 layers of DSSCs. In order to get perfect charge separation between dye molecules and HTM phases, polymeric HTM should be organized in the pores as hole conductors that nicely contact with dye molecules adsorbed on the nc-TiO_2 surface. A sophisticated route is to *in situ* synthesize HTM polymers within the nanopore of the dyed nc-TiO_2 electrode.

TABLE 1. PEDOT-Based DSSCs: Configuration and Performances[a]

device no.	sensitizer/anion doped in PEDOT/metal on FTO cathode	additive in DSSC	J_{sc} (mA cm^{-2})	V_{oc} (V)	FF	η (%)
1	N-719/*p*-toluenesulfonate/Pt	nothing	0.048	0.34	0.33	0.054[b]
2	N-719/*p*-toluenesulfonate/Pt	EMIm-TFSI and LiTFSI with TBP	0.068	0.44	0.41	0.12[b]
3	N-719/ClO_4/Au	EMIm-TFSI and LiTFSI with TBP	1.8	0.46	0.38	0.31
4	Z-907/ClO_4/Au	EMIm-TFSI and LiTFSI with TBP	3.7	0.79	0.73	2.1
5	Z-907+DCA/ClO_4/PEDOT	BMIm-TFSI and LiTFSI with TBP	4.5	0.85	0.69	2.6
6	HRS-1/ClO_4/Au	EMIm-TFSI and LiTFSI with TBP	4.5	0.78	0.74	2.8

[a] Measured under one sun conditions. [b] Oxidative polymerization using Fe(III) tris-*p*-toluenesulfonate as a oxidation catalyst.

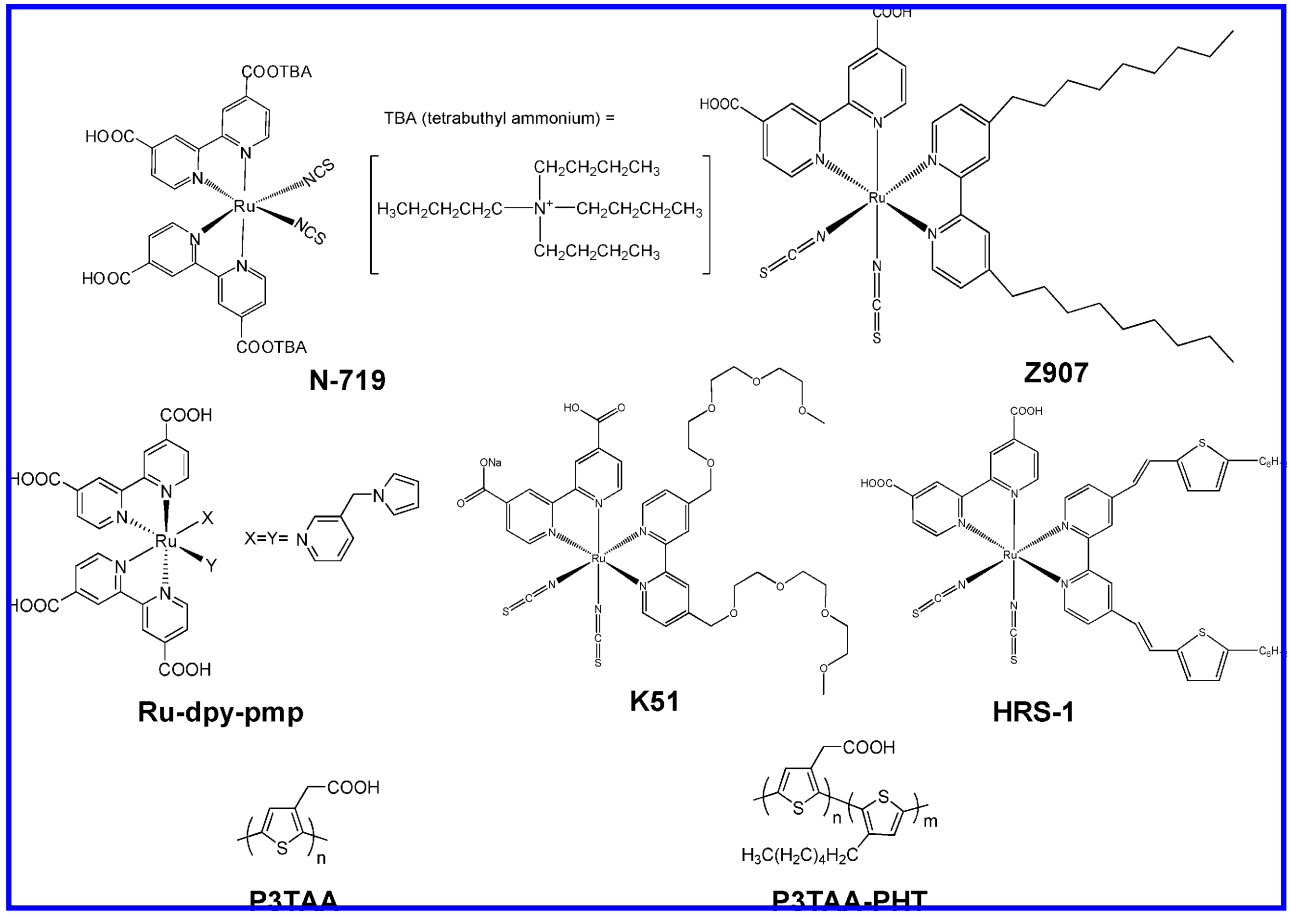

FIGURE 4. Sensitizers employed for HTM-based DSSCs.

The authors' group reported for the first time the construction of polypyrrole-based DSSC as a iodide/iodine-free DSSC.[35] For pore filling of polypyrrole into the pores of the N3 dye-adsorbed nc-TiO_2 layer, *in situ* photoelectrochemical polymerization (PEP) of pyrrole was achieved but gave very poor conversion efficiency (Table 1). The photovoltaic performance, however, was improved by introduction of lithium perchlorate ($LiClO_4$) in device layers. Further, the cell characteristics were slightly improved (J_{sc} = 0.07 mA cm^{-2}, V_{oc} = 630 mV under reduced light intensity (22 mW/cm^2) when N3 dye was replaced by oleophilic dye, $Ru(dcb)_2(pmp)_2$ (pmp = 3-(pyrrole-1-ylmethyl)-pyridine) as a sensitizer (Ru-bpy-pmp) in Figure 4).[35]

The *in situ* PEP can be successfully applied to effective pore filling of PEDOT in porous nc-TiO_2 voids by employing the more oxidizable bis-ethylenedioxythiophene (bis-EDOT, E_{ox} = 0.5 V vs Ag/Ag$^+$) instead of EDOT (E_{ox} = 1.0 V vs Ag/Ag$^+$). The preliminary experiments revealed, however, that the conversion efficiency was very poor when our newly developed polymeric polythiophene molecules, P3TAA and P3TAA-PHT (Figure 4), were employed as sensitizers for volatile solvent-free solid-state PEDOT-based DSSC.[36]

Cyclic voltammetry analysis in the dark and under irradiation elucidated that the excited Ru dye, Z-907 molecules indeed play a key role in the *in situ* PEP processes.[37] Figure 5 shows the corresponding cyclic voltammograms obtained for

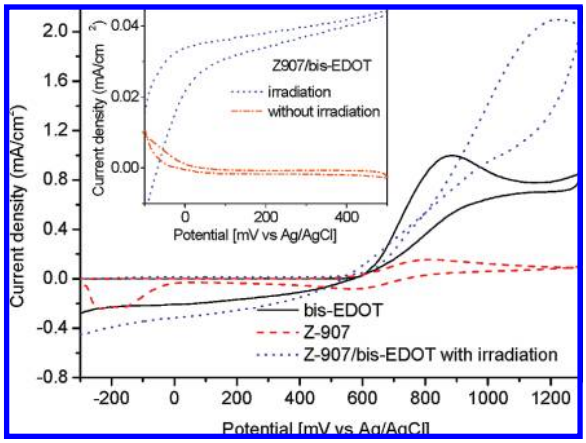

FIGURE 5. Cyclic voltammograms of bis-EDOT, Z-907, and Z-907/bis-EDOT with or without irradiation. (The inset is the comparison of the irradiation effect on the Z-907/bis-EDOT mixed system. Supporting electrolyte: 0.1 M $LiClO_4$ in acetonitrile.)

the monomer bis-EDOT and the Z-907-anchored nc-TiO_2 using a 1 cm^2 area of the FTO/nc-TiO_2/dye on FTO as the working electrode in acetonitrile solution of $LiClO_4$ as electrolyte. In the dark, the onset of bis-EDOT oxidation potential (0.605 V vs SCE) is observable around 600 mV, while the onset oxidation potential for the Z-907 is around 500 mV. These relations indicate that the electrochemical polymerization of bis-EDOT must be carried out at potentials above the oxidation limit for the dye Z-907 to suppress oxidative degradation of the dye. Under illumination conditions, however, the Z-907/bis-EDOT shows an important current response in the range between 0 and 500 mV. In order to analyze this effect, we examined the cyclic voltammograms in the voltage range between −100 and +500 mV (see the inset of Figure 5) and observed respective increases in current from zero to 20−40 μA when shifting from the dark into illumination conditions.

Accordingly, PEP was carried out under potentiometric conditions in a three-electrode one-compartment electrochemical cell using the dye-adsorbed nc-TiO_2 electrode as the working electrode, Pt wire as the counter electrode, and Ag/AgCl as the reference electrode. The external potential, 0.2 V vs Ag/AgCl, gives the best performance for PEP of bis-EDOT. Further investigation of the PEP technique revealed that the dye excitation from the cathode side irradiation gave better conversion efficiency than that from the anode side irradiation. Figure 6 shows that the PEP process is triggered by the photoexcitation of the ruthenium dye, leading to the formation of a PEDOT chain with close contact to the dye molecules.

Figure 7 shows an assembled cell structure, FTO/blocking layer/nc-TiO_2/dye-moleucles/PEDOT/catalytic cathode, and chemical structures of the ruthenium dye molecules examined. In Table 1, the cell performance data of representative PEDOT-based DSSCs are shown, where dye molecules, additives, and catalysts on cathode FTO are shown as exemplified.

Devices 1 and 2 were fabricated by the *in situ* thermal polymerization of EDOT in the presence of a catalyst, Fe(III) tris-*p*-toluenesulfonate and imidazole in *n*-butanol.[38] The formed PEDOT can be expressed as PEDOT/Tos, where the doped PEDOT is shown as a delocalized structure (Figure 3). They gave a very poor conversion efficiency even after treatment with 1-ethyl-3-methylimidazolium bis(trifuluoromethylsulfonyl)imide (EMIm-TFSI) containing *tert*-butylpyridine (TBP) (0.2 M) and lithium bis(trifuluoromethylsulfonyl)imide (LiTFSI) (0.2 M). The presence of imidazolium and lithium cation should have contributed to enhancement of electron diffusion of the nc-TiO_2 electrode.

When the PEP method was introduced using bis-EDOT as a stating monomer and the hydrophobic ruthenium dye Z-907, the short circuit photocurrent J_{sc} is dramatically increased.[39] In addition, the respectable V_{oc} of the PEP-based DSSC was always obtainable, suggesting the effective suppression of electron recombination at the TiO_2/Z-907/PEDOT interfaces. These facts imply that the PEP method contributes to unidirectional electron flow especially at the PEDOT/hydrophobic dye interfaces.

Figure 8 shows comparison of diffusion coefficients and lifetime between PEDOT-based and iodide/iodine-based DSSCs using Z-907 as dye molecules. The diffusion coefficients in the PEDOT-based DSSC are larger than those in the iodide/iodine-base DSSC, being in agreement with the remarkable fill factor due to the conductivity of the PEDOT. The decreased lifetime may be due to the recombination of the injected electrons in nc-TiO_2 to the dye molecules that are not covered enough with PEDOT.

As for the distribution of PEDOT, the volume and the average chain length of the formed PEDOT can be roughly calculated from the degree of polymerization, the density of PEDOT (1.34 g cm^{-3}), and the porosity of the TiO_2 layer (0.53 for the films made of Nanoxide-T). For example, the ratio of the volume occupied by PEDOT in mesoporous nc-TiO_2 layers was given as ca. 20%, and the average chain length based on homogeneous polymerization from each dye molecule was ca. 6.8 EDOT units under the conditions of the polymerization charge of 25 mC cm^{-2} and TiO_2 thickness of 5 μm. These calculations indicate that the PEDOT filling in devices should be essential to increase J_{sc} as high as possible.

The coadsorption of Z-907 with deoxycholic acid (DCA) (device 5) resulted in improvement of J_{sc} up to 4.5 mA cm^{-2}, suggesting that the well-organized Z-907 molecules on nc-TiO_2 layers should contribute to smooth infiltration of bis-

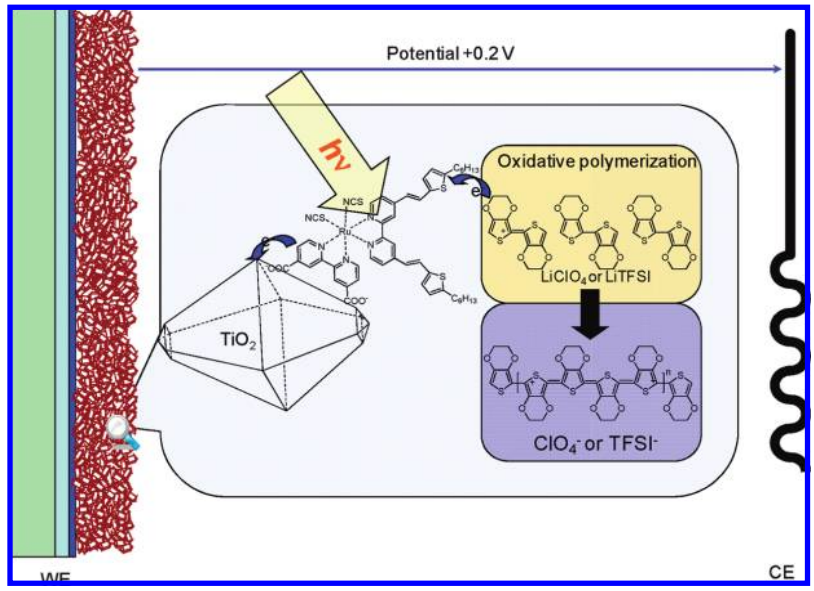

FIGURE 6. Schematic of PEP of bis-EDOT at potentiometric conditions.

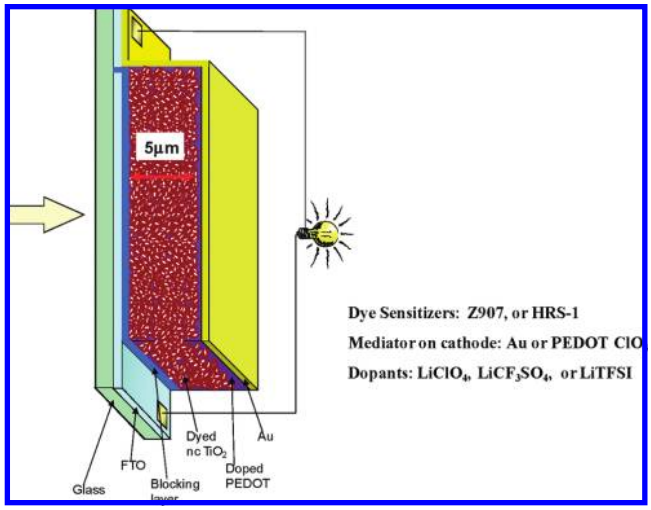

FIGURE 7. Cell configuration of effective PEDOT-based DSSC.

EDOT into the oleophilic nanopore and the resulting favorable nonbonding contact with the *in situ* formed PEDOT polymer chains.[40] It is worth mentioning that PEDOT/*X* (Figure 3, $X = ClO_4$) prepared on the cathode side FTO by chronoamperometry of 0.8 V vs Ag/Ag^+ in the presence of $LiClO_4$ electrolyte worked as well as the gold catalytic mediator on the cathode FTO.

3.3.2. Performance Optimization. The crucial strategy toward high performance of PEDOT-based DSSCs is the complete coverage of PEDOT on the dye-anchored nc-TiO_2 surface and noncovalent bonding but electronic contact of the PEDOT with dye molecules in nc-TiO_2 electrodes. The authors' group expected that the nonbonding electronic contact could be achieved by employment of a new dye, *cis*-Ru[4,4′-di(hexylthienylvinyl)-2,2′-bipyridyl] (4,4′-dicarboxylic acid-2,2′-bipyridyl)$(NCS)_2$ (HRS-1),[41] because the thienyl groups in dye molecule should self-organize bis-EDOT at interfaces through $\pi-\pi$ stacking bonding (Figure 4, device 6 in Table 1).

The optimization studies cleared the following facts.[42] (1) The total polymerization charge (~15 mC cm^{-2}) changes within only a few percent by changing the TiO_2 layer thickness (d = 3.2, 5.8, and 8.5 μm). (2) The short circuit current density reaches the highest value (on average 4.5 mA cm^{-2}) when the TiO_2 layer is 5.8 μm, and the fill factor increases significantly by increasing the TiO_2 thickness up to 5.8 μm while the open circuit voltage varies only slightly with the TiO_2 thickness. Then the highest power conversion efficiency of 2.6% is achieved with the 5.8 μm-thick nc-TiO_2 layer. (3) The current density−voltage (*IV*) curves for the device with a 5.8 μm thick nc-TiO_2 layer at various illumination intensities and the photovoltaic parameters plotted versus the light intensity (Figure 9) indicate a linear light intensity dependence of the short circuit current. The maximum efficiency of these devices is reached at the highest measured light intensities. (4) The power conversion efficiency depends on short circuit current density (J_{sc}). Even though a larger fraction of the incoming photon is absorbed when the thickness (d) is increased, J_{sc} increases only slightly. These observations indicate insufficient PEDOT coverage of the HRS-1 molecules on the nc-TiO_2 electrodes.

3.3.3. PEP-Derived PEDOT Infiltration and Their Interface Buildup. PEDOT-based DSSCs using Z-907 as a sensitizer were analyzed by sets of PEP experiments using $LiClO_4$, $LiCF_3SO_3$, $LiBF_4$, and LiTFSI as dopant.[37] The photoelectrochemical polymerization charge (mC cm^{-2}), conductiv-

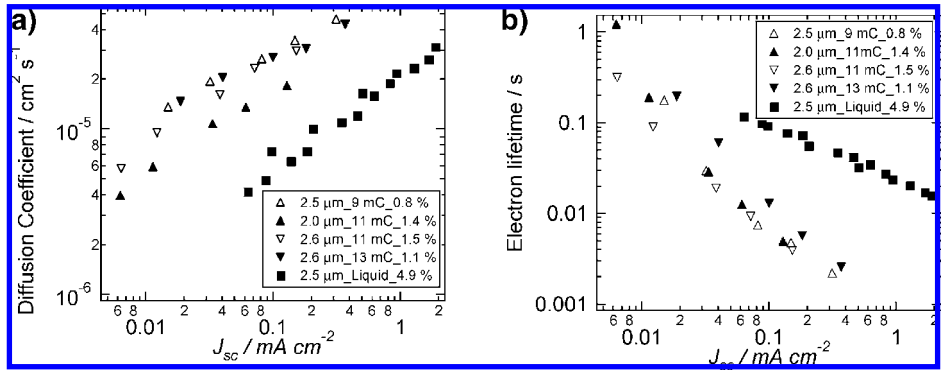

FIGURE 8. Electron diffusion coefficients and electron lifetimes: (a) Electron diffusion coefficients in TiO_2 electrode of PEDOT-based DSSC (triangles) or iodide-based DSSC (squares) as a function of J_{sc}. Inset shows the thickness of the TiO_2 layer, the polymerization charge of PEDOT, and the energy conversion efficiency at AM1.5 irradiation. All samples show the power law dependence on J_{sc}. (b) Electron lifetimes in the TiO_2 electrode of PEDOT-based DSSC (triangles) and iodide-based DSSC (squares) under open circuit conditions as a function of J_{sc}.

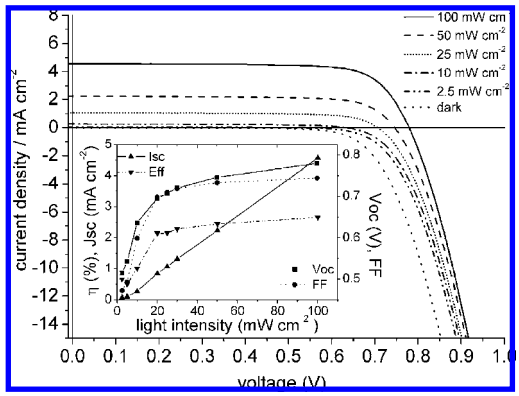

FIGURE 9. Current density vs voltage curves at various light intensities of a PEP-derived PEDOT-based DSSC: TiO_2 layer thickness is 5.8 μm. Inset shows the light intensity dependence of the short circuit current (J_{sc}), open circuit voltage (V_{oc}), filling factor (ff), and power conversion efficiency (η).

ity ($\acute{o}$), series resistance (R_s), and shunt resistance (R_{sh}) were compared with the corresponding conversion efficiency. The PEDOT/LiTFSI system gave the highest conductivity and the highest degree of polymerization charge, which was increased by about 50% higher than those of other systems. Thus, the conductivity observed for the PEDOT layer is directly dependent on the doping anion species, decreasing in the order of $TFSI^- > CF_3SO_3^- > ClO_4^- > BF_4^-$ (Table 2, Figure 3).

The high conductivity of the LiTFSI-doped PEDOT (PEDOT/*X*, *X* = TFSI in Figure 3) could be explained in terms of charge delocalization of the TFSI anion; that is, the most delocalized TFSI anion will induce preferred stacking of the charge localized (soft) polaronic cluster of the transverse PEDOT. Moreover, PEDOT/LiTFSI shows the lowest R_s and highest R_{sh}, whereas PEDOT/$LiBF_4$ shows the highest R_s with the lowest R_{sh} (see Table 2). The increase of R_s arises from the resistance of the cell material to current flow and from resistive contacts, and the decrease of R_{sh} arises mainly from leakage of current at the oxidized dye molecules on nc-TiO_2. Thus, it is not surprising that the application of the PEDOT layer with higher conductivity (i.e., the PEDOT/LiTFSI system) presents the lowest series resistance (R_s) and the highest shunt resistance (R_{sh}) of the DSSC.

3.3.4. Impedance Analysis of Interfaces in PEDOT-Based DSSC.[37] The above-mentioned PEDOT-based DSSCs were analyzed by focusing on the interfaces via electrochemical impedance spectroscopy. Figure 10 shows Cole−Cole plots of the PEDOT-based DSSCs and a fitted Bode phase angle (Figure 10b) of experiments carried out under dark conditions at −700 mV. The results are based on the equivalent circuit shown as the inset in Figure 10a. The equivalent circuits of DSSC can be represented by two RC circuits connected in series. Two semicircles were observed in the measured frequency range of 10^{-1}−10^5 Hz for all PEDOT-based DSSC. The semicircles in the frequency regions 10^3−10^5 and 1−10^3 Hz correspond to charge-transfer processes occurring at the Au/PEDOT interface and the FTO-TiO_2/dye/PEDOT interface, respectively. The first semicircle (R_1) is larger than that obtained from using organic or ionic liquid electrolytes, which means that the charge transport at the Au/PEDOT interface is

TABLE 2. Effect of Doped Anions on PEP, Conductivity of PEDOT, and Performance of PEDOT-Based DSSC

device no.	doped anion as lithium salt	PEP charge (mC cm^{-2})	conductivity (S cm^{-1})	J_{sc} (mA cm^{-2})	V_{oc} (V)	ff	R_s (Ω)	R_{sh} (kΩ)	η (%)
7	ClO_4	10.7	30	3.6	0.69	0.72	97.2	8.36	1.8
8	TFSI	15.8	130	5.3	0.75	0.73	48.3	25.6	2.9
9	$LiCF_3SO_4$	10.7	86	4.8	0.64	0.71	60.4	4.47	2.2
10	$LiBF_4$	9.5	7.5	2.8	0.51	0.63	121	2.65	0.9

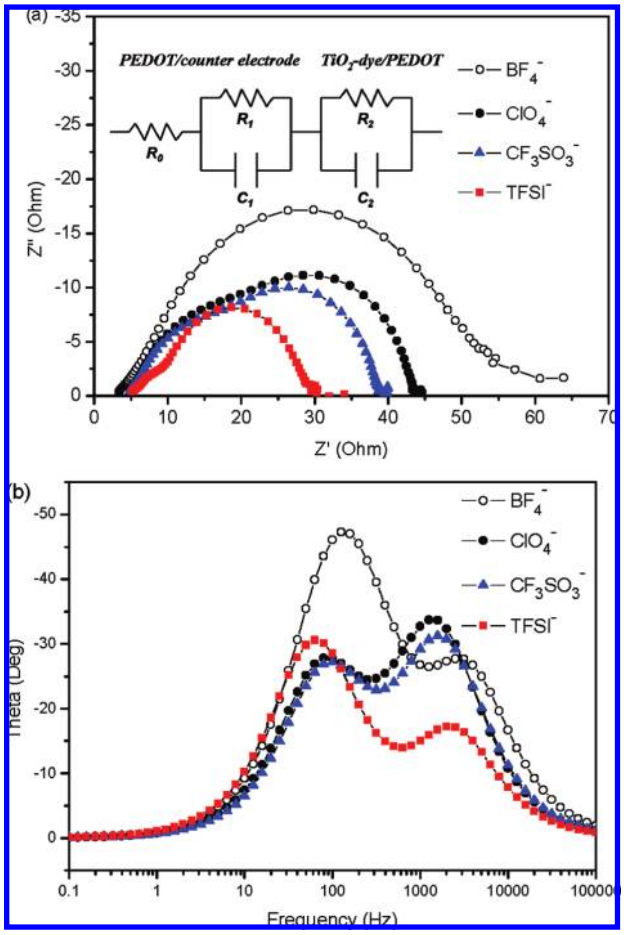

FIGURE 10. Electrochemical impedance spectra of PEDOT-based DSSC with different doping anions: $TFSI^-$ (square), $CF_3SO_3^-$ (triangle), ClO_4^- (solid circle), and BF_4^- (open square). (a) Nyquist plots; (b) fitted Bode phase plots.

TABLE 3. Parameters Obtained by Fitting the Impedance Spectra of PEDOT-Based DSSCs Shown in Figure 10a Using the Equivalent Circuit

	R_0 (Ω cm^2)	R_1 (Ω cm^2)	C_1 (F cm^{-2})	R_2 (Ω cm^2)	C_2 (F cm^{-2})
BF_4^-	3.88	4.45	1.51×10^{-5}	45.0	6.80×10^{-5}
ClO_4^-	5.61	11.1	1.64×10^{-5}	25.8	1.31×10^{-4}
$TFSI^-$	5.72	4.02	2.10×10^{-5}	19.7	2.23×10^{-4}
$CF_3SO_3^-$	5.59	9.63	1.56×10^{-5}	22.8	1.31×10^{-4}

more difficult in PEDOT-based DSSCs than that at the I^-/I_3^-/Pt interface in the iodine-based DSSC.

Table 3 reveals that the $LiBF_4$-doped PEDOT system and the LiTFSI -doped PEDOT system show similar R_1 values, indicating a good contact between PEDOT and the Au metal electrode. Nevertheless, the $LiBF_4$-doped PEDOT system shows the worst conversion efficiency. The latter is reflected in the different values of R_2 obtained; that is, the $LiBF_4$-doped PEDOT system gave the highest R_2 value, while the LiTFSI-doped PEDOT system shows the lowest one, which is in good agreement with the reversed order observed for the conversion efficiency. The latter results indicate that the TFSI-doped PEDOT exhibits an excellent charge transfer between the PEDOT layer and the Z-907 molecules on nc-TiO_2, which will be understood as being due to nonbonding oleophilic contact between them, which leads to the lowered series resistance coupled with the good hole-conducting property.

As suggested previously, the ratio of the volume occupied by PEDOT in the $LiClO_4$-doped PEDOT-based Z-907-sensitized DSSC was given as ca. 20%, which means that the PEDOT-vacant nanospace and the PEDOT-untouched dye molecules would be electron leakage sites once the devices have higher J_{sc}. It would be expected that the porosity of nc-TiO_2 electrodes should be optimized and the control of the nanospace would be crucial for the PEDOT pore filling.

4. Conclusions

On the basis of understanding the liquid I^-/I_3^- redox shuttle in conventional DSSCs, research on iodide/iodine-free DSSCs was reviewed, and we summarize as follows: (1) In the case of liquid-type iodide/iodine-free DSSCs, that is, metal complex redox shuttles, the redox couple medium must be in balance with the charge-transporting ability as well as match with the energy structure of dye sensitizers as observed by the light-intensity driven decrease in J_{sc} of the DSSC. (2) With regard to solid-state iodide/iodine-free DSSCs using a polymeric HTM, not only energetic matching of the HTM with dye molecules but also the mobility of the HTM and dyed nc-TiO_2 layers must be balanced. Lithium and/or imidazolium ions are indispensable as additives for keeping high electron diffusion of nc-TiO_2 layers. (3) As for the infiltration of solid HTM into nanopores of the nc-TiO_2 layers, the priority is optimization of the thickness of nc-TiO_2 layers, which may depend on the porosity of the nc-TiO_2 layer. The thinner the thickness is, the better the infiltration is. (4) The key issue for successful iodide/iodine-free DSSCs is the buildup of well-organized interfaces that create nonbonding but electronic contact with one another at nc-TiO_2/sentizier/HTM and HTM/cathode. Overviews of figures of structures of the sensitizers that are successfully employed with the metal complex shuttles and HTM indicate that oleophilic interactions between them play a hopeful role in iodide/iodine-free DSSCs. (5) PEP is the best method for fabrication of iodide/iodine-free PEDOT-based DSSCs. The PEP technique is applicable to effective pore filling of the thicker porous layer ($d = \sim 5$ μm) than the spin-coating technique ($d = \sim 2$ μm). The PEP-derived DSSCs are characterized by increased conductivity of PEDOT layers and

by nonbonding contact of PEDOT chains and dye molecules as depicted in the Conspectus graphic.

This work was partly supported by NEDO project under the ministry of Economy, Trade and Industry in Japan and Grant-in-aid for Scientific and Research (20750150), and NSFC (20774103, 5062351, U0634004) and 973 Program (2006CB806200 and 2006CB93100).

BIOGRAPHICAL INFORMATION

Professor Shozo Yanagida became an emeritus professor of Osaka University in 2004. He is now a full-time guest professor at the Center for Advanced Science and Innovation, Osaka University. More than 15 years have passed since he started research on photosynthetic dye-sensitized solar cells as silicone-free environment-friendlier photovoltaics.

Dr. Youhai Yu studied materials physics and chemistry, and undertook his Ph.D. in the Department of Chemistry at Jilin University, under the supervision of Prof. Wanjin Zhang. After 2 years at Jilin University as a Research Assistant for Prof. Zhang and half a year as a postdoctoral research assistant at the Korea Advanced Institute of Science and Technology, he joined Prof. Yanagida's group in April 2007 as a NEDO postdoctoral fellow to start his photovoltaic research at the Center for Advanced Science and Innovation, Osaka University.

Dr. Kazuhiro Manseki completed his Ph.D. under the supervision of Prof. Masatomi Sakamoto in 2002 (University of Yamagata, Japan). From 2001 to 2002, he was a Research Fellow of the Japan Society for the Promotion of Science (JSPS). After working as researcher in a company, he joined Osaka University as a postdoctoral fellow in 2003 and has studied luminescent materials in the laboratory of Professor Shozo Yanagida. He became Specially Appointed Assistant Professor of the Center for Advanced Science and Innovation, Osaka University, in 2008, being promoted to Guest Associate Professor in 2009.

FOOTNOTES

* To whom correspondence should be addressed. E-mail: s.yanagida@casi.osaka-u.ac.jp.

REFERENCES

1 Grätzel, M. Photoelectrochemical cells. *Nature* **2001**, *414*, 338–344.
2 Xia, J.; Yanagida, S. Strategy to improve the performance of dye-sensitized solar cells: Interface engineering principle. In *Progress in Solar Energy, A Technical Review Journal*; Yogi Groswami, D., Ed.; Elsevier, in press.
3 Benkö, G.; Kallioinen, J.; Korppi-Tommola, J. E. I.; Yartsev, A. P.; Sundström, V. Photoinduced ultrafast dye-to-semiconductor electron injection from nonthermalized and thermalized donor states. *J. Am. Chem. Soc*. **2002**, *124*, 489–493.
4 Könenkamp, R. Carrier transport in nanoporous TiO_2 films. *Phys. Rev. B* **2000**, *61*, 11057–11064.
5 Matsui, H.; Okada, K.; Kitamura, T.; Tanabe, N. Thermal stability of dye-sensitized solar cells with current collecting grid. *Sol. Energy Mater. Sol. Cells* **2009**, *93*, 1110–1115.
6 Kawano, R.; Watanabe, M. Equilibrium potentials and charge transport of an I_2/I_3^- redox couple in an ionic liquid. *Chem. Commun*. **2003**, 330–331.
7 Chiba, Y.; Islam, A.; Watanabe, Y.; Komiya, R.; Koide, N.; Han, L. Y. Dye-sensitized solar cells with conversion efficiency of 11.1%. *Jpn. J. Appl. Phys., Part 2* **2006**, *45*, L638–L640.
8 Kubo, W.; Murakoshi, K.; Kitamura, T.; Yoshida, S.; Haruki, M.; Hanabusa, K.; Shirai, H.; Wada, Y.; Yanagida, S. Quasi-solid-state dye-sensitized TiO_2 solar cells: effective charge transport in mesoporous space filled with gel electrolytes containing iodide and iodine. *J. Phys. Chem. B* **2001**, *105*, 12809–12815.
9 Hagfeldt, A.; Grätel, M. Molecular photovoltaics. *Acc. Chem. Res*. **2000**, *33*, 269.
10 Nusbaumer, H.; Moser, J.-E.; Zakeeruddin, S. M.; Nazeeruddin, M. K.; Grätzel, M. Co(dbbip) complex rivals tri-iodide/iodide redox mediator in dye-sensitized photovoltaic cells. *J. Phys. Chem. B* **2001**, *105*, 10461.
11 Sapp, S. A.; Elliot, C. M.; Contado, C.; Caramori, S.; Bignozzi, C. A. Substituted polypyridine complexes of cobalt(II/III) as efficient electron-transfer mediators in dye-sensitized solar cells. *J. Am. Chem. Soc*. **2002**, *124*, 11215–11222.
12 Hattori, S.; Wada, Y.; Yanagida, S.; Fukuzumi, S. Blue copper model complexes with distorted tetragonal geometry acting as effective electron-transfer mediators in dye-sensitized solar cells. *J. Am. Chem. Soc*. **2005**, *127*, 9648–9654.
13 Oskam, G.; Bergeron, B. V.; Meyer, G. J.; Searson, P. C. Pseudohalogens for Dye-Sensitized TiO_2 Photoelectrochemical cells. *J. Phys. Chem. B* **2001**, *105*, 6867–6873.
14 Kopidakis, N.; Schiff, E. A.; Park, N.-G.; van de Lagemaat, J.; Franck, A. J. Ambipolar diffusion of photocarriers in electrolyte-filled nanoporous TiO_2. *J. Phys. Chem. B* **2000**, *104* (16), 3930–3936.
15 Kambe, S.; Nakade, S.; Kitamura, T.; Wada, Y.; Yanagida, S. Influence of the electrolytes on electron transport in mesoporous TiO_2—electrolyte systems. *J. Phys. Chem. B* **2002**, *106*, 2967–2972.
16 Tennakone, K.; Kumara, G. R. R.; Kottegoda, I. R. M.; Wijayantha, K. G. U.; Perrera, V. P. S. A solid-state photovoltaic cell sensitized with a ruthenium bipyridyl complex. *J. Phys. D: Appl. Phys*. **1998**, *31*, 1492–1496.
17 Sirimanne, P. M.; Jeranko, T.; Bogdanoff, P.; Fiechter, S.; Tributsch, H. On the photo-degradation of dye sensitized solid-state TiO_2|dye|CuI cells. *Semicond. Sci. Technol*. **2003**, *18*, 708–712.
18 Kumara, G. R. A.; Konno, A.; Shiratsuchi, K.; Tsukahara, J.; Tennakone, K. Dye-sensitized solid-state solar cells: Use of crystal growth inhibitors for deposition of the hole collector. *Chem. Mater*. **2002**, *14*, 954–955.
19 O'Regan, B.; Schwartz, D. T.; Zakeeruddin, S. M.; Grätzel, M. Electrodeposited nanocomposite n-p heterojunctions for solid-state dye-sensitized photovoltaics. *Adv. Mater*. **2000**, *12*, 1263–1267.
20 Kumara, G.; Konno, A.; Senadeera, G. K. R.; Jayaweera, P. V. V.; De Silva, D.; Tennakone, K. Dye-sensitized solar cell with the hole collector p-CuSCN deposited from a solution in n-propyl sulphide. *Sol. Energy Mater. Sol. Cells*. **2001**, *69*, 195–199.
21 O'Regan, B.; Lenzmann, F.; Muis, R.; Wienke, J. A Solid-State Dye-sensitized solar cell fabricated with pressure-treated P25-TiO_2 and CuSCN: Analysis of pore filling and IV characteristics. *Chem. Mater*. **2002**, *14*, 5023–5029.
22 Bandara, L.; Weerasinghe, H. Solid-state dye-sensitized solar cell with p-type NiO as a hole collector. *Sol. Energy Mater. Sol. Cells*. **2005**, *85*, 385–390.
23 Bach, U.; Lupo, D.; Comte, P.; Moser, J. E.; Weissortel, F.; Salbeck, J.; Spreitzer, H.; Grätzel, M. Solid-state dye-sensitized mesoporous TiO_2 solar cells with high photon-to-electron conversion efficiencies. *Nature* **1998**, *395*, 583–585.
24 Snaith, H. J.; Zakeeruddin, S. M.; Wang, Q.; Pchy, P.; Grätzel, M. Dye-sensitized solar cells incorporating a "liquid" hole-transporting material. *Nano Lett*. **2006**, *6*, 2000–2003.
25 Sicot, L.; Fiorini, C.; Lorin, A.; Nunzi, J.-M.; Raimond, P.; Sentein, C. Dye sensitized polythiophene solar cells. *Synth. Met*. **1999**, *102*, 991–992.
26 Gebeyehu, D.; Crabec, J. B.; Sariciftci, N. S.; Vangeneugden, D.; Kiebooms, R.; Vanderzande, D.; Kienberger, F.; Schindler, H. Hybrid solar cells based on dye-sensitized nanoporous TiO_2 electrodes and conjugated polymers as hole transport materials. *Synth. Met*. **2002**, *125*, 279–287.
27 Spiekermann, S.; Smestad, G.; Kowalik, J.; Tolbert, L. M.; Grätzel, M. Poly(4-undecyl-2,2′-bithiophene) as a hole conductor in solid state dye sensitized titanium dioxide cells. *Synth. Met*. **2001**, *121*, 1603–1604.
28 Grant, C. D.; Schwartzberg, A. M.; Smestad, G. P.; Kowalik, J.; Tolbert, L. M.; Zhang, J. Z. Characterization of nanocrystalline and thin film TiO_2 solar cells with poly(3-undecyl-2,2′-bithiophene) as a sensitizer and hole conductor. *J. Electroanal. Chem*. **2002**, *522*, 40–48.
29 Al-Dmour, H.; Taylor, D. M.; Cambridge, J. A. Effect of nanocrystalline-TiO_2 morphology on the performance of polymer heterojunction solar cells. *J. Phys. D: Appl. Phys*. **2007**, *40*, 5034–5038.
30 Kudo, N.; Honda, S.; Shimazaki, Y.; Ohkita, H.; Ito, S. Improvement of charge injection efficiency in organic-inorganic hybrid solar cells by chemical modification of metal oxides with organic molecules. *Appl. Phys. Lett*. **2007**, *90*, 183513-1–183513-3.
31 Wang, Z. J.; Qu, S. C.; Zeng, X. B. Hybrid bulk heterojunction solar cells from a blend of poly(3-hexylthiophene) and TiO_2 nanotubes. *Appl. Surf. Sci*. **2008**, *255*, 1916–1920.

32 Jiang, K.-J.; Manseki, K.; Yu, Y.-H.; Masaki, N.; Xia, J.-B.; Yang, L.-M.; Song, Y.-L.; Yanagida, S. Photovoltaics Based on Hybridization of Effective Dye-Sensitized Titanium Oxide and Hole-Conductive Polymer P3HT. *Adv. Funct. Mater*. **2009**, *19*, 2481–2485.

33 Zhu, R.; Jiang, C.-Y.; Liu, B.; Ramakrishna, S. Highly efficient nanoporous TiO_2 - polythiophene hybrid solar cells based on interfacial modification using a metal-free organic dye. *Adv. Mater*. **2009**, *9*, 994–1000.

34 Li, Y. X.; Hagen, J.; Haarer, D. Novel photoelectrochromic cells containing a polyaniline layer and a dye-sensitized nanocrystalline TiO_2 photovoltaic cell. *Synth. Met*. **1998**, *94*, 273–277.

35 Murakoshi, K.; Kogure, R.; Wada, Y. Yanagida, Fabrication of solid-state dye-sensitized TiO_2 solar cells combined with polypyrrole. *Sol. Energy Mater. Sol. Cells*. **1998**, *55*, 113–125.

36 Senadeera, R.; Norihiro, F.; Saito, Y.; Kitamura, T.; Wada, Y.; Yanagida, S. Volatile solvent-free solid-state polymer-sensitized TiO_2 solar cells with poly(3,4-ethylenedioxythiophene) as a hole-transporting medium. *Chem. Commun*. **2005**, *17*, 2259–2261.

37 Xia, J.-B.; Masaki, N.; Lira-Cantu, N.; Kim, Y.; Jiang, K.-J.; Yanagida, S. Influence of doped anions on poly(3,4-ethylenedioxythiophene) as hole conductors for iodine-free solid-state dye-sensitized solar cells. *J. Am. Chem. Soc*. **2008**, *130*, 1258–1263.

38 Saito, Y.; Azechi, T.; Kitamura, T.; Hasegawa, Y.; Wada, Y.; Yanagida, S. Photo-sensitizing ruthenium complexes for solid state dye solar cells in combination with conducting polymers as hole conductors. *Coord. Chem. Rev*. **2004**, *248* (13—14), 1469–1478.

39 Fukuri, N.; Masaki, N.; Kitamura, T.; Wada, Y.; Yanagida, S. Electron transport analysis for improvement of solid-state dye-sensitized solar cells using poly(3,4-ethylenedioxythiophene) as hole conductors. *J. Phys. Chem. B* **2006**, *110*, 25251–25258.

40 Kim, Y.; Sunga, Y.-N.; Xia, J.-B.; Lira-Cantu, N.; Masaki, N.; Yanagida, S. Solid-state dye-sensitized TiO_2 solar cells using poly(3,4-ethylenedioxythiophene) as substitutes of iodine/iodide electrolytes and noble metal catalysts on FTO counter electrodes. *J. Photochem. Photobiol. A* **2008**, *193*, 77–80.

41 Jiang, K.-J.; Masaki, N.; Xia, J.-B.; Noda, S.; Yanagida, S. A novel ruthenium sensitizer with a hydrophobic 2-thiophen-2-yl-vinyl-conjugated bipyridyl ligand for effective dye sensitized TiO_2 solar cells. *Chem. Commun*. **2006**, *23*, 2460–2462.

42 Mozer, A. J.; Wada, Y.; Jiang, K.-J.; Masaki, N.; Yanagida, S.; Mori, S. N. Efficient dye-sensitized solar cells based on a 2-thiophen-2-yl-vinylconjugated ruthenium photosensitizer and a conjugated polymer hole conductor. *Appl. Phys. Lett*. **2006**, *89*, 043509.